كلية الهندسة بشبرا
FACULTY OF ENGINEERING AT SHOUBRA
ERJ
PRINT ISSN 3009-6049
ONLINE ISSN 3009-6022

ENGINEERING RESEARCH JOURNAL (ERJ)
Volume (53) Issue (3)
Jul. 2024, pp:91-102
https://erjsh.journals.ekb.eg

Structural Response of Ultra-High-Performance Concrete (UHPC) Columns under Eccentric Loads

M. Abdelkarim[1*], A. Nabil[1],Mohamed S. Saif[1], Gehan Hamdy[1], Hossam Z. El-Karmoty[2], M. O. Ramadan[1]

[1] Department of Civil Engineering, Faculty of Engineering at Shoubra, Benha University, Cairo, Egypt
[2]Housing & Building National Research Institute (HBRC).
[*] Corresponding Author.
E-mail: **Mahmoud.abdelkareem@feng.bu.edu.eg, mohamed.ismaeel@feng.bu.edu.eg, Osama.alhariri@feng.bu.edu.eg, Gehan.hamdy@feng.bu.edu.eg, Hoskarmoty@yahoo.com, ahmed.khater@feng.bu.edu.eg**

Abstract: The research investigates the structural response of ultra-high-performance concrete (UHPC) columns under eccentric compression using experimental and nonlinear finite element analysis (NLFEA). Eight slender UHPC columns with an average concrete compressive strength of 133 MPa were tested under eccentric loading. The main experimental variables were**:** column slenderness ratio (6, 12, and 18), load**-**eccentricity ratio (0.1, 0.2, and 0.5), and the inclusion of a 2% volumetric ratio of steel fibers. Performance metrics such as failure pattern, load-lateral displacement relationship, ductility, and steel reinforcement strain were used to assess the columns' behavior. ANSYS15 is used to develop NLFEA for the tested columns. The column ultimate load and mid-height lateral displacement analytical results have an average difference of 3.75% and 23%, respectively, when compared to experimental results. The results showed that high slenderness ratios or high load-eccentricity ratios reduce column load-carrying capacity but enhance ductility and crack patterns. Short, low eccentric columns experienced sudden failure, where 1.4% of stirrups failed to confine the column core after the spalling of the concrete cover. The inclusion of 2% steel fibers restrained the spalling and crushing of the slender UHPC columns and enhanced the column ductility.

KEYWORDS: ultra-high-performance concrete columns, eccentric uhpc columns, slender uhpcc, and steel fiber effect on uhpc columns

1. Introduction

Ultra-high-performance concrete (UHPC) is a composite material characterized by its superior mechanical characteristics. It has superior compressive strength (120 to 200 MPa), an improved modulus of elasticity, a high density, enhanced dimensional stability, reduced permeability, and notable resistance to chemical attack. In addition, it has a high workability in its fresh state. It was first launched in the early 1990s using a high cement content, a high content of supplementary cementitious materials (SCMs), and fine aggregate with a significantly low water-to-binder ratio (w/b) less than 0.20. Meanwhile, significant progress has been made in the field of chemical additive development to reduce the water content during the mixing process (Naaman, 2012). Most UHPCs were designed using refined aggregate grading. This is to avoid the coarse aggregate's intrinsic strength limit and overcome the coarse aggregate. Also, to prevent the paste matrix's inherent weakness, increase homogeneity, and eliminate stress concentration at the points of contact between those aggregates [2-3]. The development of UHPC using different mix designs and techniques, or even using different SCMs, is still the main headline of much research. Of course, it is an attractive concrete type with superior characteristics. However, it hasn't been registered in the construction industry as expected until now due to its uneconomical costs. The uneconomical costs are not limited to material costs; they are also due to the special requirements in the mixing and curing processes. Recently, with the help of aggregate backing particle models, basalt aggregates were combined to enhance UHPC mixes. According to Rozalija and Darwin (K. Rozalija, 1997), the inherent strength of the rock is the reason why high-strength concrete with basalt aggregate yields better mechanical properties than high-strength concrete with limestone. Coarse aggregate can lower costs, alter the workability of UHPC more readily, and increase the elastic modulus, according to Ma et al. (J. Ma, 2004). Li et al. [6] reported that the coarse basalt aggregate has a limited reduction effect on the mechanical strength

of UHPC. The optimal powder content of about 800 kg/m^3 and 700 kg/m3 are found for UHPC when the maximum basalt aggregate size is 8 mm and 16 mm, respectively. Moreover, the addition of double-headed short steel fibers enhances the strain-hardening behavior of uniaxial tension due to bridging actions. [7-8]. Fibers' inclusion also creates a confining effect. The confinement allows UHPC to demonstrate significantly greater strength retention and compression ductility in comparison to traditional high-strength concrete materials. All these features and the cost-effectiveness of the newly developed UHPC make it the first choice for developing concrete columns, reducing its cross sections, and increasing the carrying load capacities in high-rise buildings.

To omit coarse aggregate from UHPC, Hosinieh et al. [9] and Shin et al. [10] conducted an experimental investigation on the pure compressive axial behavior of UHPC short columns. These experiments showed that load-bearing capabilities and load sustainability after peak were significantly improved by reducing the gap between the transverse reinforcements of the short column for a certain percentage of transverse reinforcement volumetric ratios. Moreover, Hosinieh, et al. [9] remarked that adding more crossties for the transverse reinforcements would merely improve the overall toughness of the short columns without appreciably increasing their load-bearing capacity due to the unchanged stirrup spacing. Meanwhile, the steel fibers' presence helped to effectively regulate the spalling of the concrete at failure, which in turn improved the columns' post-peak ductility. Shin et al. [10] reported that the obtained ultra-high strength up to 180 MPa for columns would require a transverse reinforcement ratio of approximately 10% as per ACI 318-14 [11] provisions for seismic, leading to steel congestion and concrete casting problems. His research findings indicate that the use of hybrid short steel fibers reinforcement by 1.5% proved to be successful in partially eliminating confinement reinforcement. Steven and Empelmann [12] and Hung et al. [13] studied the behavior of short UHPC columns under eccentric loading, Steven and Empelmann [12] considered an average concrete strength of 150 MPa with eccentric loading ratios varied between 2% to 30%, while Hung et al. [13] used a concrete strength of 100 MPa and a constant eccentricity ratio of 130%. The experimental findings indicated a superior load-carrying capacity for columns when compared to conventional concrete columns. The outer concrete fibers of column cross sections cracked at strain 3% without steel fiber and up to 3.2% for columns that contain 1.5% short steel fiber [12]. The short slender HPC columns' ability to resist spalling and crushing was successfully inhibited by the addition of steel fibers with a volume percentage of 0.75% or higher. Specifically, a 70% reduction in 3.5% confinement reinforcement may be compensated for by adding a 1.5% volume fraction of steel fiber, all the while maintaining the slender columns' ductility under eccentric stress [13].

In response to the desired development in the UHPC field where the basalt aggregates are re-added, Hung and Yen [14] examined the compressive behavior of twelve UHPC short columns eleven of them with coarse aggregate, it was concluded that the initial stiffness of the UHPC columns was found to be little affected by both the transverse reinforcement and the fiber content. Additionally, the use of coarse aggregate in the HPC columns significantly increased the secant stiffness by nearly 100%. It enhanced the structural integrity of the columns by altering the damage pattern, resulting in the formation of rougher spalling surfaces and more tortuous cracks. Furthermore, incorporating 1.5% of steel fibers allows for the substitution of fifty percent of the transverse reinforcement mandated by the code, while effectively averting premature buckling of longitudinal bars subjected to axial loads.

Employing newly developed UHPC in place of traditional concrete materials in reinforced concrete columns is approved to improve both the design and performance of centric-loaded columns [15]. However, more research is needed to fully understand the behavior of these UHPC components regarding eccentrically loaded slender columns. Using UHPC material allows concrete columns' cross-sectional dimensions to be significantly reduced, but the increased slenderness impact may negatively affect the columns' behavior. Due to its interaction with the axial load, or the P-Delta effect, the non-negligible slenderness effect will amplify the lateral displacement and moment demand of the slender UHPC columns. This could result in the slender UHPC columns having a lower load-resistant capacity. The previous studies on eccentric columns focused on column confinement parameters, either transverse tie percentage, arrangement, or steel fiber content. It shall be highlighted that these studies were limited to UHPC without basalt aggregate and ignored the slenderness effect. In response, the current study examined the behavior of reinforced slender UHPC columns under eccentric-loading with basalt aggregate addition. The impact of several design parameters, such as the eccentricity ratio, slenderness ratio, and the presence of short, discontinuous steel fibers, on the columns' performance was investigated. A 3-D finite element analysis using ANSYS 15 is conducted to simulate the experimental results.

2. EXPERIMENTAL PROGRAM

2.1 Columns specimens

A total of eight ultra-high-performance concrete (UHPC) column members were fabricated at the construction yard attached to the Housing and Building National Research Center, Egypt. All the columns had the same cross-section (150 x 150) mm with an enlarged thickness of 300mm at column ends to facilitate or for ease of application of eccentric-load as per Figure 1. Also, reinforcement configuration was identical for all columns where the longitudinal reinforcement at the critical mid-height portion is 4T10 (1.4%) with Y6@50mm (1.2%) transverse reinforcement. Near the column ends, an additional longitudinal bar is added at the tension side and the spacing of stirrups is reduced to 30mm to prevent local failure beneath the loading plates. The clear cover was kept to 15mm per each side using spacers. Figure 2 shows the column's formwork and reinforcement cages before pouring.

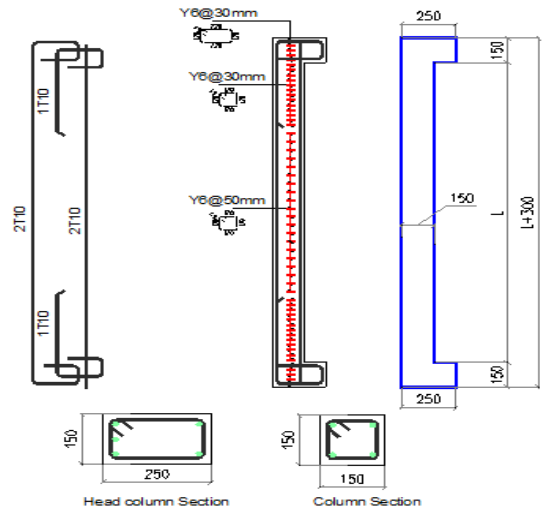

Fig 1: Geometry and Reinforcement Details of Columns.

Fig 2: Columns Formwork and Reinforcement Cages

2.1. *Materials*

Table 1 summarizes the proportions either in kg/m^3 or by volumetric percentage for the two mixes of the UHPC material that was used in the current investigation. The primary ingredients of mix A were Type I ordinary Portland cement, limestone powder, silica fume, metakaolin, and silica sand with a maximum aggregate of 1.18mm, basalt coarse aggregate with a maximum aggregate size of 10 mm, water, and polycarboxylate-based superplasticizer (Guillenium 888). A total of 2% of short steel fibers measuring 30 mm in length, 0.38 mm in diameter, 201 GPa elastic modulus, and 3070 MPa nominal yield strength are included in the other mix. The UHPC materials were designed to have a 135 MPa compressive strength after 90 days. The columns were reinforced with D10 and D6 steel bars that had a nominal yield strength of 500 MPa and 280 MPa, respectively. Table 2 provides an overview of the steel reinforcements' actual tensile characteristics, which were determined by direct tensile testing.

Table 1: UHPC Components for Mixes A and B.

Mix	C	Ls	S	M	FA	BA	W	SP	SF	B	W/B
A	496 (15.8)	164 (5.1)	110 (6.2)	54 (2.2)	752 (28.4)	750 (25)	158 (15.8)	16.8 (1.5)	-	825 (29.3)	0.20
B	486 (15.4)	161 (5)	108 (6.1)	53 (2.1)	737 (27.8)	735 (25)	155 (15.5)	16.5 (1.5)	157 (2)	809 (28.7)	0.20

C=Cement, Ls=Limestone, S=Silica Fume, M=Metakaolin, FA=Sand Fine Aggregate, BA= Basalt aggregate, W=Water, SP=Super-plasticizer, and B= total binder content.

Table 2: Measured Mechanical Properties for Reinforcing Bars.

Size	Grade	Yield Strength (MPa)	Ultimate Strength (MPa)	Elongation (%)
6mm	B280C-P	305	453	22.8
10mm	B500DWR	537	685	16.3

Table 3: HPC Columns Test Matrix.

Groups	Column	Material type	f_{cu} (MPa)	Height (H) mm	Ecc. (e) mm	Slenderness (H/D)	Ecc. Ratio (E/D)
Group I, II	6C15	A	132	900	15	6	0.1
Group I	12C15	A	138	1800	15	12	0.1
	18C15	A	131	2700	15	18	0.1
Group II	6C37	A	141	900	37.5	6	0.25
	6C75	A	132	900	75	6	0.5
Group III	6Cs15	B	128	900	15	6	0.1
	6Cs75	B	129	900	75	6	0.5
	18Cs15	B	131	2700	15	18	0.1

2.2. *Columns design*

The tested columns have a constant cross-section of (150x150) mm, 1.4% longitudinal reinforcement ratio (4T10), and 1.2% transversal reinforcement (Y6@50mm), while The column members' primary design variables, as per Table 3, were the following: (1) slenderness factor; (2) eccentricity ratio; and (3) incorporation of 2% short steel fibers. The slenderness factor (h/L) is the ratio between the clear height (L) and the column cross-section depth (h). Three slenderness factors are considered in the current investigation 6, 12, and 18 correspond to clear heights 900mm, 1800mm, and 2700mm. The eccentricity ratios (e/h) were considered to be 10%, 25%, and 50% and correspond to absolute eccentricities (e) of 15mm, 37.5mm, and 75mm. The eccentricity and the slenderness parameters were covered by five columns, where the control column 6H15 was common in each parameter. Additional Three columns (6Cs15, 6Cs75, and 18Cs15) were considered to assess the effect of fiber inclusion in combination with eccentricity and slenderness effect.

2.3Test instrumentation and load protocol

The compressive strength, f_{cu}, of the UHPC materials, was obtained using three compressive tests on 100 mm × 100 mm x100 concrete cubes for each column. The compressive tests were conducted according to ASTM C109 (C109, 2004) and BS EN 12390 3:2019 [17]. The tensile behavior was studied for each UHPC mix by performing indirect tensile tests either by Brazilian indirect tension test per ASTM C496 (C496, 2017) on three cylinders 100mm diameter x150mm length or by three-point flexure test per ASTM C293 (C293, 1994) on beams 100mmx100mmx 500mm. The material compressive tests were carried out either 24 hours before or after the testing of the relevant column member. The representative material attribute was determined by averaging the three test results.

With the configuration depicted in Figure 3, the columns were tested under eccentric loading. Eccentric compressive loads were applied to the columns at a rate of around 7 kN/s using hydraulic press loading equipment with a 5000 kN capacity. The boundary conditions of the tested columns reflected hinged conditions at both ends. Where, the two ends of each column member were pin linked to steel connectors fixed to a strong floor and a hydraulic actuator, respectively. The pin connections allowed free rotation in the test plane of the column while constraining the degrees of freedom. It should be noticed that the rough face of the column, from which the concrete was cast, was purposefully pointed in the direction of the out-of-plane test to minimize the effect of surface irregularity on test results. At least six Linear Variable Differential Transducers (LVDTs) were used to instrument each column. Five LVDTs, of 0.001 mm accuracy, were distributed along the column height in-plane direction to track the lateral displacement curve of the column in-plane, while one LVDT, of 0.001 mm accuracy, was set in the mid-height of the perpendicular direction to record if there is an existing deformation at the out-of-plane side. The axial displacement was measured by a machine laser tool. Near or at column mid-height, at least four electrical strain gages having 10 mm length were attached to longitudinal and transverse steel at mid-height and were connected to the data logger indicator to observe strains of steel directly. They were arranged by the role of two by two, two for the tension side and the other for the compression side for both longitudinal and transversal reinforcement.

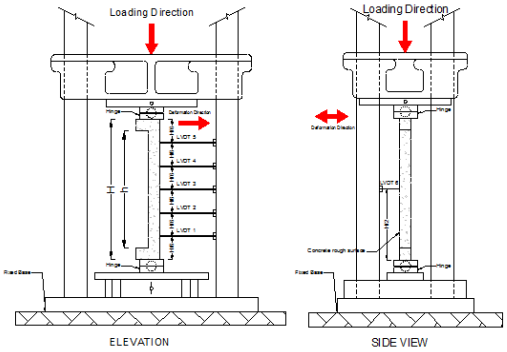

Fig 3: Elevation and Side View of Typical Columns Lateral Displacement Instrument Setup (LVDT).

4.2. Test results and discussion

Tested columns 6C15, 12C15, and 18C15 were characterized by explosive failure at the compression zone without any remarkable cracks. The main difference was the failure zone location, column 18C15 failed at the mid-height, while columns 6C15 and 12C15 failed on the lower third as shown in Figure 4. As the eccentricity increased the first crack was noticed, and a tension crack was remarked for Columns 6C37.5 and 6C75 at 85%, and 53% of their final loads, respectively. For group three columns where 2% of short steel fibers were added, the failure explosive sound disappeared, and columns maintained their concrete covers. Column 6Cs15 failed at the lower end and the shear crack pattern was noticed over a considerable time in a ductile manner as per Figure 5. The first crack appeared at 89% of its final load. Column 18Cs15 failed near its mid-height under the growth of a single perpendicular bending moment crack initiated at 81% of its failure load, while a pattern of bending cracks formed for column 6Cs75, and the first crack initiated at 56% of its failure load.

Fig 4: Columns Failure Pattern.

Fig 5: Shear Failure Pattern of Column 6Cs15.

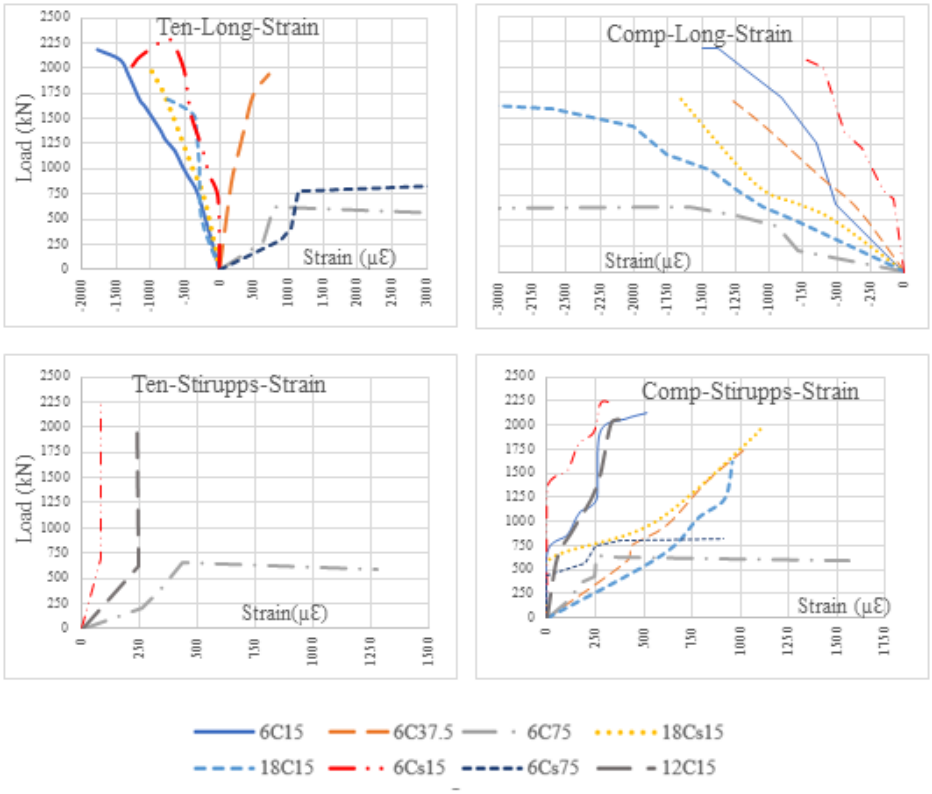

Fig 6: Strain Of Longitudinal and Transverse Reinforcement.

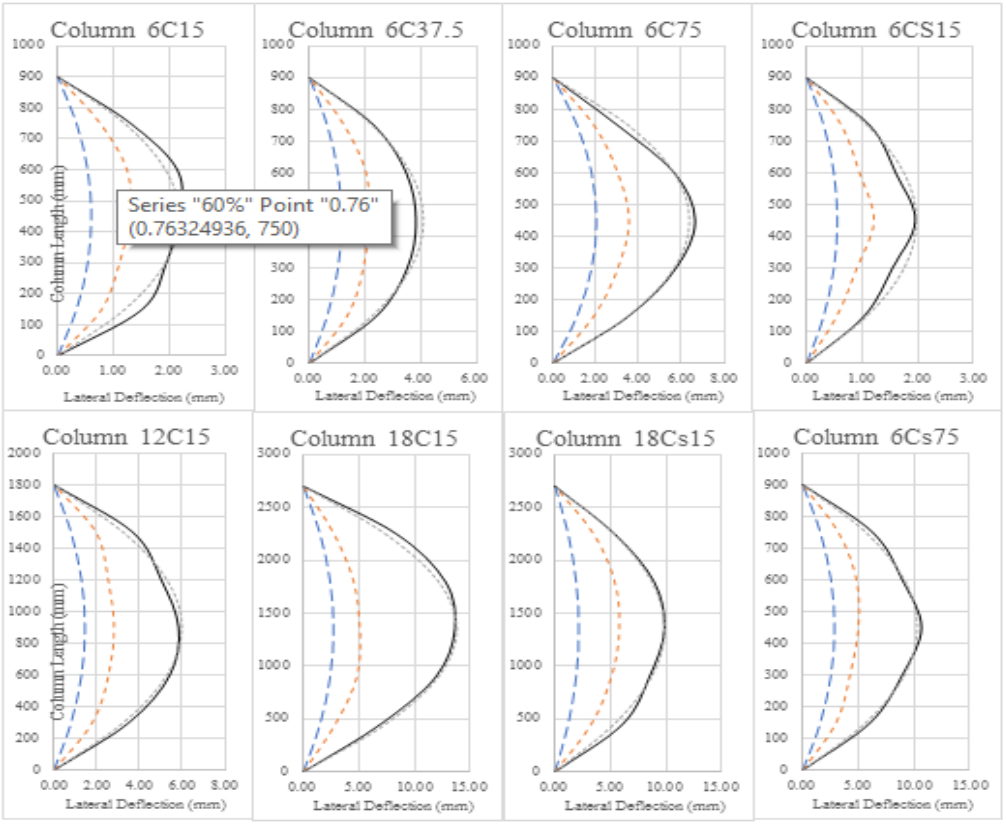

Fig 7: Columns Lateral Displacement At 30%, 60% And 100% of The Maximum Experimental Failure Loads.

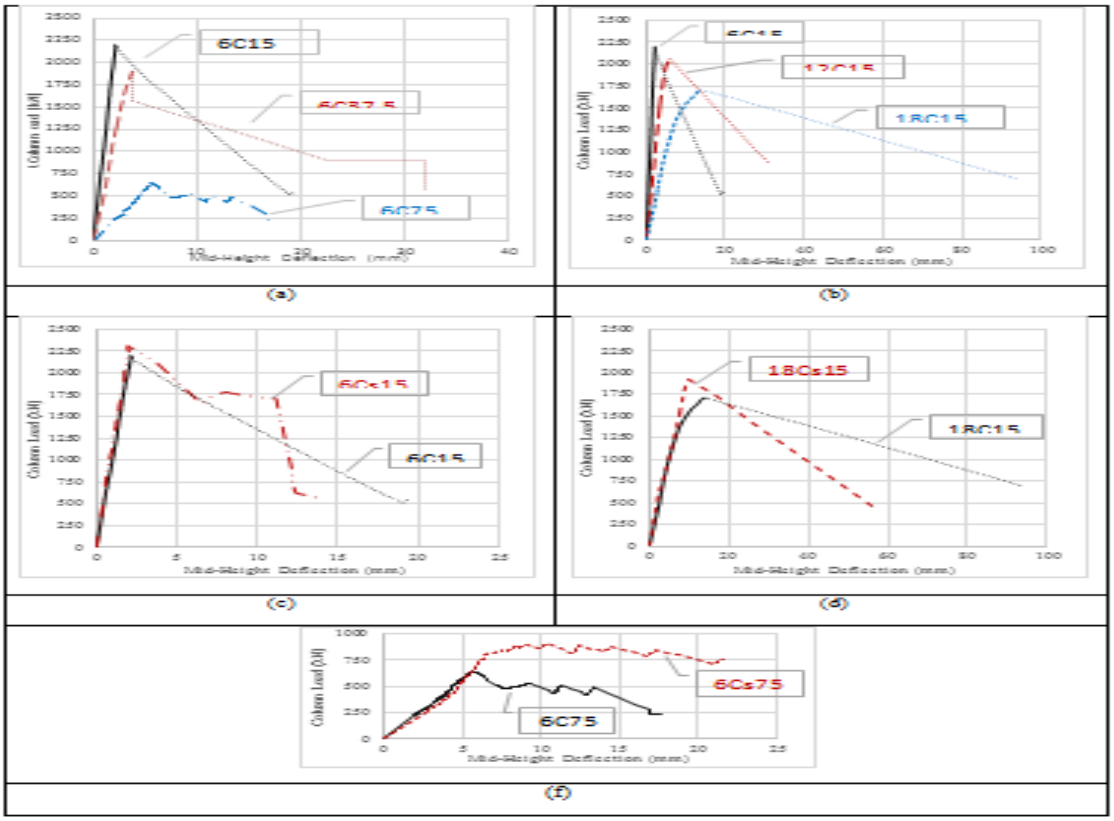

Fig 8: Columns Load Versus Mid-Height Lateral Displacement Response

4.2. Effect of the load-eccentricity

Group II is designed to study the effect of load-eccentricity. It contains control columns 6C15, 6C37.5, and 6C75, with eccentricities of 0.1, 0.25, and 0.5 of column thickness, respectively. Columns having an eccentricity ratio less than or equal to 0.25 (6C15 and 6C37.5) were brittle under explosive failure, while column 6C75 failed in tension failure with a remarkable crack pattern. Figure 8 shows the response of columns under different eccentricity ratios. Where the degradation of the post-peak curve for column 6C37.5 was less steep than column 6C15, while column 6C75 showed a realistic ductile manner. The load-carrying capacity for column 6C37.5 is less than 6C15 by 14% while it is higher than column 6C75 by 110%, this is shared between the effect of load eccentricity and the increased compressive strength for this column. As the eccentricity of the applied loads increased, the depth of the compressed zone at mid-height decreased. This is the subsequent of the increased strain gradient, compressive strains at the column tension side are reduced by the effect of increased eccentricity and turn to be tensile strains for an eccentricity ratio of 0.25 or more. At Column 6C15, the entire cross-section was under compression, while the recorded strains at tension sides for columns 6C37.5 and 6C75 are 0.0013 and 0.00175, respectively. Specimens subjected to large load-eccentricity 6C37.5, and 6C75 showed greater mid-height lateral displacement at the ultimate load of 75%, and 201%, respectively, than columns subjected to small load-eccentricity 6C15. The same observation is recorded for columns 6Cs15 and 6Cs75, where the mid-height lateral displacement of column 6Cs75 increased by 474%. The ultra-high increase in the mid-height lateral displacement for column 6Cs75 is not limited to the increase in the eccentricity ratio, the existence of short steel-headed fibers increases the bridging action and resists the cracks propagation which allows more pre-peak ductile behavior. The degradation of loads for column 6Cs75 was less steep after peak loads than 6Cs15 which explains the extension of the post-peak stage longer than the referenced column.

4.3. Effect of slenderness ratio

Group I is designed to study the effect of slenderness ratios. It consists of 6C15, 12C15, and 18C15, with slenderness ratios of 6, 12, and 18, respectively, which corresponds to clear heights of 900mm, 1800mm, and 2700mm. Examination of columns with heights near the traditional typical story height is a unique topic for this research. The load-carrying capacity is reduced by increasing the column slenderness ratio due to the P-delta effect, the column curvature increases and is accompanied by subsequent increases in mid-height lateral displacement. Each increase in the mid-height lateral displacement means an additional moment that creates the effect of strain gradient. Typically, the existence of the strain gradient limits the compressive zone and reduces the carrying load capacity. Columns 12C15 and 18C15 ultimate loads are less than the reference column 6C15 by 6%, and 28%, respectively, while the mid-height lateral displacement increased by 166% and 522% in the same sequence. Increasing the strain gradient effect reduces the post-peak degradation slope. The same remarks concluded when comparing columns 6Cs15 with column 18Cs18, the reduction in load-carrying capacity is 20% with an increase in the mid-height lateral displacement by 404%.

4.4. Effect of the addition of steel fibers

Group III was cast using material B, where 2% of short steel fibers are added, incorporation of steel fibers increases the concrete resistance to tension forces, increases the initial column stiffness, and enhances the column ductility. The initial column stiffness of columns 6Cs15 and 18Cs15 are higher than columns 6C15 and 18C15 which reduces the mid-height lateral displacement by 11% and 28% , respectively. The limited mid-height lateral displacement reflected an increase in the load-carrying capacity by 5% and 12.7%, respectively. On the other hand, a 39.2% increase in the load-carrying capacity was recorded for column 6Cs75 when compared to column 6C75. The superior enhancement in the load-carrying capacity accompanied by an increase in the mid-height lateral displacement by 55% is due to the enhanced concrete tension capacity. The steel fibers resist the cracks propagation and increase tensile strain capacity. All columns of group III have a highly ductile manner even with short low eccentric column 6Cs15.

5. ANALYTICAL STUDY

All tested columns described in Table 3 were modeled by Using a non-linear finite element analysis program, ANSYS15, to check the applicability of such analytical tools for predicting the UHPC column's response. 3D solid element SOLID65 is used to simulate UHPC response, Columns of Groups I&II and Group II had two different concrete definitions, one for concrete cover and the other for confined core. Columns of group III are defined by using a fibers-smeared approach. The behavior of concrete in compression is idealized using Légeron and Paultre [20] stress train idealizations for both confined and unconfined concrete, Figure 9-d. The behavior of concrete in tension is simplified by a tri-linear approach as per Figure 9-f. Figure 9-g describes the constitutive concrete failure surface. Steel bars were represented by the discrete model using the 3D spar link180 element. A full bond is assumed between concrete and reinforcement, where the common nodes between steel bar elements (3D LINK180) and concrete

components (SOLID65) transfer the strain effects between the two elements. A bilinear stress-strain model was used to simulate the transversal and longitudinal reinforcement behavior either on tension or in compression, Figure 9-f. To prevent stress concentration at the column boundaries, a 20mm steel plate of SOLID45 element was simulated at the column ends. Columns are pin-ended, horizontally restrained at both ends, and vertically restrained at the bottom. The restraint line is in the centroid of the direction of applied eccentricity. The failure load is the state in which there is no convergence of the solution criteria for any given force or lateral displacement**.** Figures. 9-a to f show the used elements and the stress-strain curve for the used materials. Figure 10 describes the column geometry and its bounder conditions as idealized on ANSYS.

5.2. Results of the analyzed columns

All columns showed an analytical load capacity slightly higher than experimental ones by around 5%, except columns 6Cs75, as analytical load capacity increased by 11% to the experimental result as Table 4. This is due to material defects that couldn't be idealized exactly through finite element programs. The mid-height lateral displacement is overestimated by ANSYS, especially for short low eccentric columns. The accuracy of mid-height lateral displacement is enhanced by the increased slenderness ratio or increased eccentric ratio. However, the difference in mid-height lateral displacement between analytical and experimental results shows 49% and 42% for columns 6Cs15 and 6C15, respectively. Figure 11 shows a good correlation between the experimental and analytical prediction for the mentioned columns, columns have the same ascending stiffens, and the analytical prediction showed a softening near peak results which is not the case in experimental ones. The same observation is valid for columns 12C15 and 6C37.5% in an enhanced manner where the difference in mid-height lateral displacement was 36 and 32%, respectively. Table 4 and Figure 11 show a perfect correlation for long columns (18C15 and 18Cs15) and for high eccentric columns (6C15 and 6Cs15), where the difference in mid-height lateral displacement prediction does not exceed 8%.

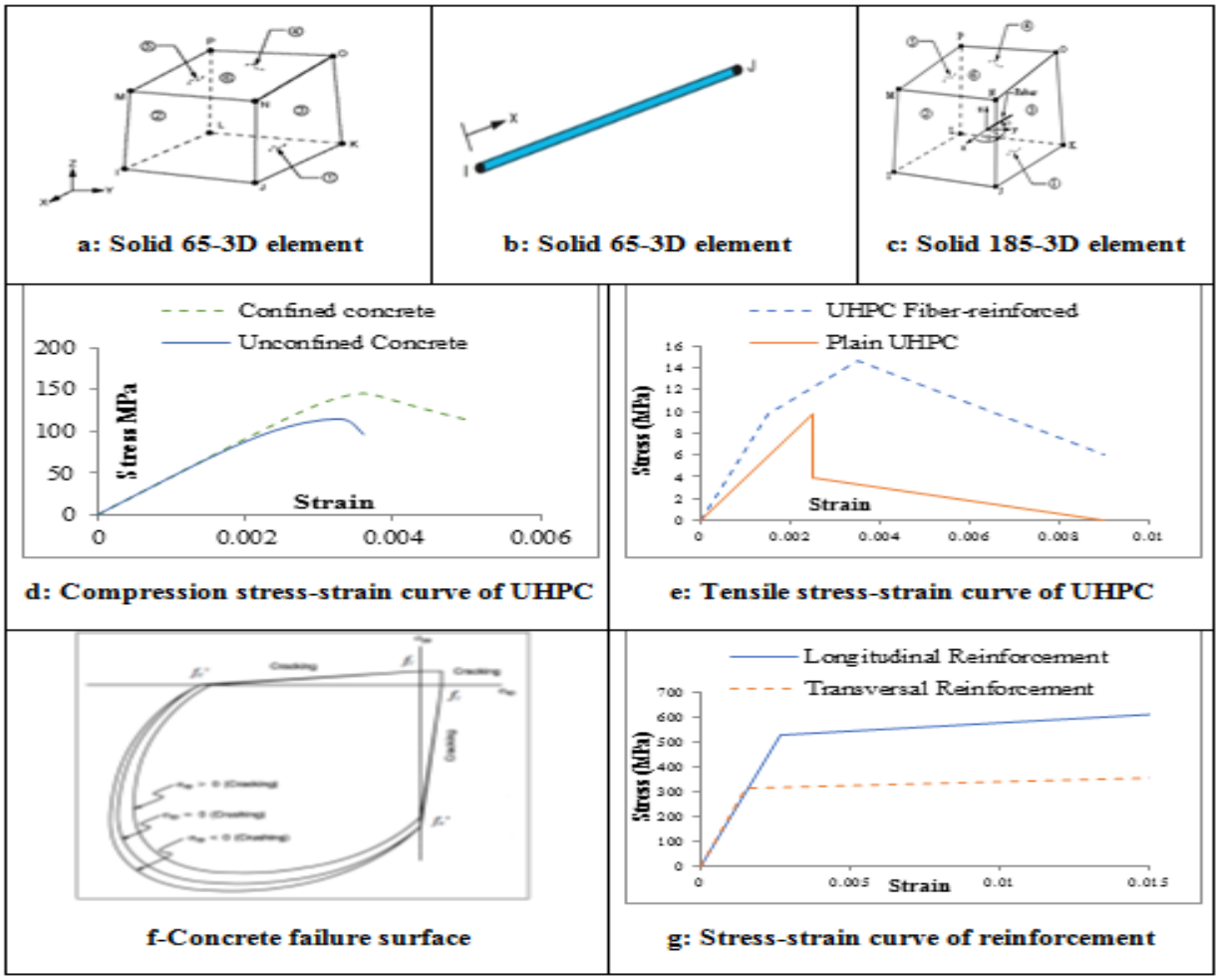

Fig 9: ANSYS Materials Constitutive Models.

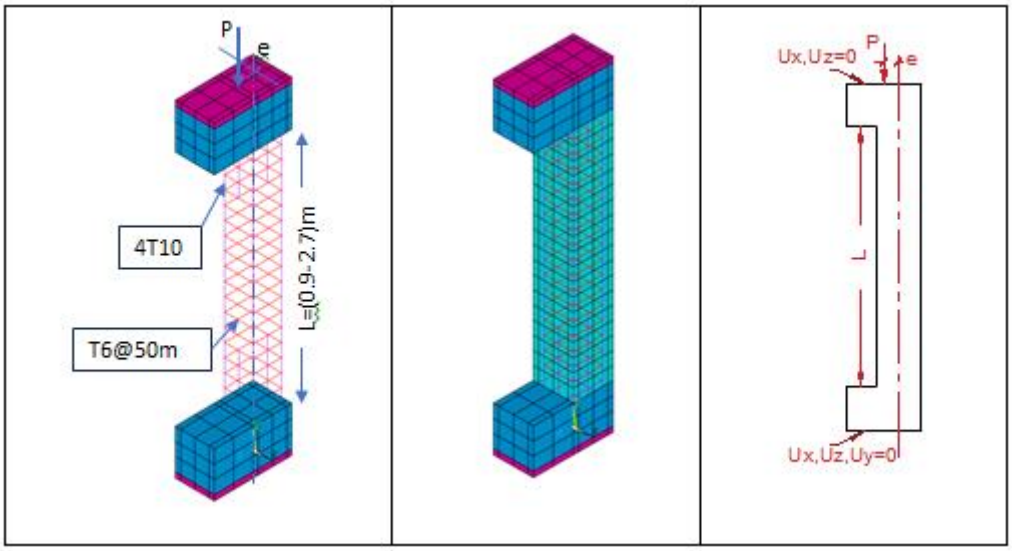

Fig 10: Column Geometry and Boundary Conditions.

Table 4: Comparison Between Experimental and Analytical Results.

Column	Group	f_{cu} (MPa)	Experimental results			Analytical results		$\frac{P_{exp}-P_{anal}}{P_{exp}}$%	$\frac{\Delta_{exp}-\Delta_{anal}}{\Delta_{exp}}$%
			P_{cr}* (kN)	P_u (kN)	Δ_u (mm) mid-height	P_u (kN)	Δ_u (mm)		
6C15	Ref.	132	-	2186.7	2.19	2196.3	3.1	-0.44	-42
12C15	Group I	138	-	2062.5	5.84	2056.3	7.95	0.30	-36
18C15		131	-	1707	13.62	1799.6	14.29	-5.42	-5
6C37	Group II	141	1614	1900	3.83	1936	5.06	-1.89	-32
6C75		132	343	647.7	6.65	667.1	7.07	-3.00	-6
6Cs15	Group III	128	2055	2311.1	1.95	2415.9	2.9	-4.53	-49
6Cs75		129	505	901.9	10.67	1000.7	11.51	-10.95	-8
18Cs15		131	1557	1925.2	9.85	2005.5	10.56	-4.17	-7

* P_{cr} is the first cracking load.

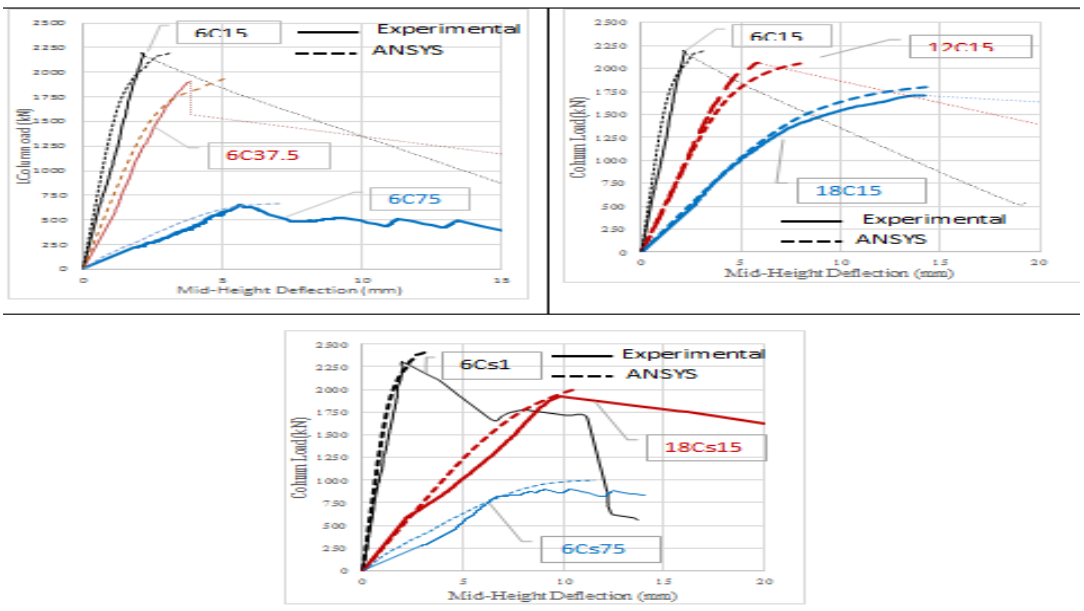

Fig 11: Comparison Between Analytical and Experimental Results for Columns Load- Lateral Displacement Response.

6.CONCLUSIONS

In this study, eight pin-ended reinforced columns (with a typical rectangular section of 150 mm ×150 mm) are manufactured using two distinct mixes of UHPC, one of them containing 2% steel fibers. The columns were loaded with an eccentric ratio e/h = (0.1,0.25 and 0.5). Three different Columns' lengths were considered, a short column of 900mm clear height, and two slender columns of lengths 1800mm and 2700mm. numerical analysis using nonlinear FE modeling (ANSYS 15) was conducted. A summary of the main study findings is listed as follows.

1- Increasing load eccentricity leads to a decrease in column load capacity, but an increase in both mid-height lateral displacement and column ductility. low eccentric columns (e/h =0.1) failed in a brittle manner without noticeable cracks. First cracks appear at 85% and 53% of ultimate loads by increasing the load-eccentricity ratio to 0.25 and 0.5, respectively. the mid-height lateral displacement of short columns was increased by 75% and 204% by increasing the eccentricity by 150% and 400%, meanwhile, a subsequent reduction in maximum load-carrying capacity of 15% and 238% was recorded.

2- Increasing the column slenderness ratio results in a decrease in load capacity, but an increase in the column mid-height lateral displacement. Increasing the column length by 100% and 200% results in an increase in the mid-height lateral displacement by 167% and 522% while the ultimate loads are reduced by 6% and 28%.

3- The addition of reinforced concrete fibers enhanced the response of eccentric slender UHPC columns in terms of column ductility and ultimate loads. The post-peak behavior was clearly recorded and showed a less steep degradation with either increasing the eccentricity ratio or slenderness ratio. Column initial stiffness increased due to bridging actions of steel fibers as the crack's propagations were restricted. The mid-height lateral displacement of columns 6Cs15 and 18Cs15 was reduced by 11% and 28%, and the ultimate loads increased by 5% and 12%, respectively.

4- The enhanced concrete tension resistance due to steel fiber addition controls the high eccentric column response, Column 6Cs75 had 40% higher ultimate loads and 60% higher mid-height lateral displacement when compared to column 6C75.

5- Analytical simulations give a very good prediction of the experimental results in terms of load capacity of UHPC columns and corresponding med-height lateral displacement with an average difference of 3.75% and 23.1%, respectively. The correlation of the results was enhanced with either increased eccentricity or slenderness.

REFERENCES

[1] A. E. Naaman and K. Wille, "The Path to Ultra-High Performance Fiber Reinforced Concrete (UHP-FRC): Five Decades of Progress," HiperMat 2012 (Kassel, March 7-9, 2012), pp. 3-15.

[2] P. Richard and M. Cheyrezy, "Composition of reactive powder concretes," Cement and Concrete Research, vol. 25, no. 7, pp. 1501-1511, 1995.

[3] D.Y. Yoo and N. Banthia, "Mechanical properties of ultra-high-performance fiber-reinforced concrete: A review," Cement and Concrete Composites, vol. 73, pp. 267-280, 2016.

[4] R. Kozul and D. Darwin, "Effects of Aggregate Type, Size, and Content on Concrete Strength and Fracture Energy," Lawrence, Kansas, 1997.

[5] J. Ma, M. Orgass, F. Dehn , D. Schmdit and N.V. Tue, "Comparative Investigations on Ultra-High Performance Concrete with or without Coarse Aggregates," in Proc. Int. Symp. Ultra High Perform. Concr. , Kassel. , 2004.

[6] P.P. Li, Q.L. Tu, and H.J.H. Brouwers, "Effect of coarse basalt aggregates on the properties of Ultra-high Performance Concrete (UHPC)," Construction and Building Materials, vol. 170, no. 649–659, pp. 649–659, 2018.

[7] J. Donnini, G. Lancioni, G. Chiappini, and V. Carinaldesi "Uniaxial tensile behavior of ultra-high performance fiber-reinforced concrete (UHPFRC): Experiments and modeling," Composite Structures, vol. 258, no. 113433, 2021.

[8] C. C. Hung, P. F. Sherif El-Tawil and A. S. H. Chao, "A Review of Developments and Challenges for UHPC in Structural Engineering: Behavior, Analysis, and Design," J. Struct. Eng. (ASCE), vol. 147, no. 9, pp. 1-19, 2021.

[9] M.M. Hosinieh, H. Aoude, W. D. Cook, and D. Mitchell "Behavior of ultra-high performance fiber reinforced concrete columns under pure axial loading," Engineering Structures, vol. 99, p. 388–401, 2015.

[10] H.O. Shin, K.H. Min, and D. Mitchell, "Confinement of ultra-high-performance fiber reinforced concrete columns," Composite Structures, vol. 176, pp. 124-142., 2017.

[11] ACI 318M-14, Building Code Requirements For Structural Concrete, American Concrete Institute, 2014.

[12] G. Steven and M. Empelmann, "Square columns made of UHPFRC with high-strength longitudinal reinforcement," FACHTHEMA, vol. 109, no. 5, pp. 344-354, 2014.

[13] C.-C. Hung, F.Y. Hu, and C.H.Yen, "Behavior of slender UHPC columns under eccentric loading," Engineering Structures, vol. 174, pp. 701-711, 2018.

[14] C. C. Hung and C.H. Yen, "Compressive behavior and strength model of reinforced UHPC short columns," Journal of Building Engineering, no. 102103, p. 35, 2021.

[15] M. Aboukifa and M.A. Moustafa "Structural and buckling behavior of full-scale slender UHPC columns," Engineering Structures-Elsevier, vol. 255, no. 113928, 2022.

[16] ASTM C109, "Standard Test Method for Compressive Strength of Cube Concrete Specimens," American Society for Testing and Materials Standard Practice C109, Philadelphia, Pennsylvania, 2004.

[17] BSEN 12390-3, "Compressive strength of test specimens for testing hardened concrete," British Standards Institution, London, 2019.

[18] *ASTM C496, "Standard Test Method for Splitting Tensile Strength of Cylindrical Concrete Specimens," American Society for Testing and Materials Standard Practice C496, Philadelphia, Pennsylvania,*

2017.

[19] *ASTM C293, "Standard Test Method for Flexural Strength of Concrete (Using Simple Beam with center-Point Loading)," American Society for Testing and Materials Standard Practice C293, Philadelphia, Pennsylvania, 1994.*

[20] *F. Légeron and P. Paultre, "Uniaxial Confinement Model for Normal- and High-Strength Concrete Columns," Journal of Structural Engineering, ASCE, vol. 129, no. 2, pp. 241-252, 2003.*